Available online at www.sciencedirect.com
SCIENCE DIRECT®
Journal of Sound and Vibration 282 (2005) 367–380
JOURNAL OF SOUND AND VIBRATION
www.elsevier.com/locate/jsvi

Modal parameter identification using response data only

Y. Zhang, Z. Zhang*, X. Xu, H. Hua

Institute of Vibration, Shock and Noise, Shanghai Jiaotong University, 1954 Huashan Road, Shanghai 200030, P.R. China

Received 14 May 2003; received in revised form 8 December 2003; accepted 23 February 2004
Available online 23 September 2004

Abstract

Order estimation and spurious mode elimination concerning the subspace identification technique are discussed in this paper. To avoid underestimating the state space model order, order estimate is given in terms of component energy index rather than matrix singular values. Component energy index is introduced to measure the energy contribution of signal components. Based on order estimation, spurious modes resulting from noise and model redundancy are indicated by an alternative stabilization diagram which reflects the variation of parameter estimates with row increments of the Hankel matrix. Two numerical examples and one experimental example on the parameter estimation of a cable-stayed bridge model are presented to demonstrate the efficacy of component energy index and the alternative stabilization diagram.

1. Introduction

The traditional identification techniques that extract modal parameters from input and output data have been well developed and widely used in engineering. However, it is often a hard task to carry out excitation in field testing of large engineering structures. To obviate such difficulties of the traditional techniques, methods of extracting modal parameters from structural response data only (blind techniques) have been deeply investigated during the past few decades [1–6]. Among these techniques, the natural excitation technique (NExT), random decrement technique (RDT), frequency domain decomposition (FDD) and stochastic subspace identification (SSI), etc., can

*Corresponding author.
E-mail address: chychangcn@yahoo.com (Y. Zhang).

0022-460X/$ - see front matter © 2004 Elsevier Ltd. All rights reserved.
doi:10.1016/j.jsv.2004.02.012

give good results [7–10]. Using structural response data only will reduce the complexity of modal testing and increase the flexibility of implementation. It is this essential feature that makes these blind techniques more attractive than the traditional ones.

Subspace identification techniques have got many engineering applications. They are based on the state space model of input/output signals and identification is realized by extracting system matrices from input/output signals or output signals only. In the formation of system matrices, the singular value decomposition (SVD) technique is usually used to filter noises and estimate the state space model order [11–15]. When extracting modal parameters with subspace identification techniques, model order should be overestimated in order to model weak signals and it is usually given in terms of singular values. Since a redundant model is used, the interference of spurious modes that result from noises and computation error occurs inevitably in estimated results. Therefore, it is necessary to completely identify and remove spurious modes. So far there have been many criteria such as MAC and MAmC, etc., that can be used to validate estimated modal parameters [16]. Besides these criteria, the stabilization diagram which reflects the variation of estimated modal parameters with model order increments is also an effective means used to indicate spurious modes and determine system order which, in practice, cannot be given simply in terms of singular values [17].

Since singular values are not always reliable to indicate model order, this paper gives a new approach to order estimation. The method estimates model order in terms of component energy index (CEI), which is presented to improve the way of order estimation, i.e. to avoid underestimating of model order. CEI can also indicate the energy contribution of signal components. Based on the estimation of model order, an alternative stabilization diagram is proposed to show the dependence of estimated parameters on the row increments of Hankel matrix and further to indicate spurious modes.

Section 2 is the introduction of subspace identification technique and the definition of CEI. The procedure of generating a stabilization diagram is presented in Section 3. Sections 4 and 5 are examples presented to demonstrate the efficacy of CEI and the alternative stabilization diagram. Concluding remarks are given in Section 6.

2. Identification from response data

Consider the following linear time invariant (LTI) system described by a discrete state space model:

$$\begin{aligned} x(k+1) &= Ax(k) + Bw(k), \\ y(k) &= Cx(k) + Dw(k), \end{aligned} \tag{1}$$

where $A \in R^{N\times N}$, $B \in R^{N\times P}$, $C \in R^{L\times N}$, $D \in R^{L\times P}$ are the system matrix, the input matrix, the output matrix and the direct feedthrough matrix, respectively. $x(k) \in R^N$ is the state vector, $y(k) = (y_1, y_2, \ldots, y_L)^{\mathrm{T}} \in R^L$ is the measured output, $w(k) \in R^P$ is the zero mean white noise vector with covariance matrix $E(w(k)w(k)^{\mathrm{T}}) = I$ and $I \in R^{P\times P}$ is the identity matrix [15]. k is the discrete time and $k \geqslant 0$. N is the model order (the LTI system order), P and L are the number of inputs and outputs, respectively.

From Eq. (1), we can obtain

$$\theta(i+1) = A\theta(i) + B\sigma(i),$$
$$r(i) = C\theta(i) + D\sigma(i), \tag{2}$$

where $r(i) = E(y(k)y^{\mathrm{T}}(k-i))$, $\theta(i) = E(x(k)y^{\mathrm{T}}(k-i))$ and $\sigma(i) = E(w(k)y^{\mathrm{T}}(k-i))$ are the second-order statistics (auto/cross-correlation), $i = 0, 1, 2, \ldots$. Note that $\sigma(i) = 0$, $\forall i \geqslant 1$ [18]; the recursive structure of Eq. (2) implies

$$R = \Gamma\Theta, \tag{3}$$

where

$$R = \begin{bmatrix} r(1) & r(2) & \cdots & r(q) \\ r(2) & r(3) & \cdots & r(q+1) \\ \vdots & \vdots & \ddots & \vdots \\ r(p) & r(p+1) & \cdots & r(p+q-1) \end{bmatrix}, \qquad \Gamma = \begin{bmatrix} C \\ CA \\ \vdots \\ CA^{p-1} \end{bmatrix},$$

$$\Theta = (\theta(1), \theta(2), \ldots, \theta(q)) \quad \text{and} \quad pL, qL > N.$$

In practice, $r(i)$ is approximated by $\hat{r}(i)$, which is estimated from finite samples, i.e.

$$\hat{r}(i) = r(i) + \text{noise}$$
$$= \frac{1}{M}\sum_{k=i}^{M+i-1} y(k)y^{\mathrm{T}}(k-i), \quad M > 0,\ i = 0, 1, 2, \ldots, \tag{4}$$

but for an ergodic process, $\hat{r}(i) \to r(i)$ as $M \to \infty$. The approximation of R, denoted as $\hat{R}$, can be obtained by replacing element $r(i)$ in R with $\hat{r}(i)$. As a result, $\hat{R}$ is contaminated by noises. In order to reduce noise contamination, SVD is adopted to remove noises from the Hankel matrix $\hat{R}$. Suppose the SVD of $\hat{R}$ is given as follows:

$$\hat{R} = [U_1\ U_2] \begin{bmatrix} \Sigma_1 & \\ & \Sigma_2 \end{bmatrix} \begin{bmatrix} V_1^{\mathrm{T}} \\ V_2^{\mathrm{T}} \end{bmatrix} = U_1\Sigma_1 V_1^{\mathrm{T}} + U_2\Sigma_2 V_2^{\mathrm{T}} \tag{5}$$

and Σ_1 has N dominant singular values that are far greater than the rest of Σ_2, then $U_1\Sigma_1 V_1^{\mathrm{T}}$ can be taken as a better approximation of R. In Eq. (5), U_1 corresponds to the signal subspace of $\hat{R}$. In terms of the shift structure of Γ, C and A can be computed as [15]

$$C = U_1(1:L, 1:N),$$
$$A = U_1^{+}(1:\alpha L, 1:N)U_1(L+1:(\alpha+1)L, 1:N), \tag{6}$$

where $U_1(1:L, 1:N)$ is the submatrix formed by rows 1–L and columns 1–N of U_1, U_1^{+} is the generalized inverse of U_1, and α is an integer satisfying $\alpha L > N$. From A and C, natural

frequencies, damping ratios and the normalized mode shapes can be given as

$$\begin{aligned}\omega_j &= |f_s \ln(\lambda_j)|,\\ \xi_j &= -\mathrm{Re}(f_s \ln(\lambda_j))/|f_s \ln(\lambda_j)|, \quad j = 1-N,\\ \phi_j &= C\gamma_j/||C\gamma_j||,\end{aligned} \tag{7}$$

where $\{\lambda_j\}$ and $\{\gamma_j\}$ are the eigenvalues and eigenvectors of A, respectively, f_s is the sampling frequency.

In general cases, however, no obvious gap exists between any two adjacent singular values due to noise contamination. Therefore, noise modes cannot be completely filtered even using singular value decomposition. In order not to lose any physical modes, especially those of small energy, U_1 should have sufficient number of columns, which will in most cases result in a redundant model and correspondingly spurious modes that belong to the redundant model but not the LTI system. To reduce the number of spurious modes, model order should be properly determined. In this paper, we use component energy index to indicate the model order. Using energy index instead of singular values is based on the fact that singular values cannot indicate the energy contribution of each mode, and consequently they cannot show which modes are of strong observability and which are of weak observability. CEI is introduced to indicate the energy contribution of each mode. The computation of CEI is based on the fact that the autocorrelation sequence $\{E(y_l(k)y_l(k-i))|i = 1, 2, 3, \ldots\}$ can be given as the superposition of exponentially decayed sequences, i.e.

$$E(y_l(k)y_l(k-i)) = \sum_{j=1}^{N} c_{jl}\lambda_j^i, \quad i = 1, 2, 3, \ldots, \ \ l = 1, \ldots, L, \tag{8}$$

where the coefficient c_{jl} $(j = 1, \ldots, N, l = 1, \ldots, L)$ is a complex and eigenvalues λ_1–λ_N are mutually distinct. Eq. (8) can be derived directly from the solution of Eq. (2) to the initial condition $\theta(0)$ and the impulse load $\{\sigma(0)\delta(i)|i = 0, 1, 2, \ldots\}$, which is of the following form [19]:

$$r(i) = D\sigma(0)\delta(i) + \sum_{j=1}^{N} \Psi_j\lambda_j^i, \quad i = 0, 1, 2, \ldots,$$

where $\delta(i)$ is the unit impulse function and Ψ_j $(j = 1, \ldots, N)$ is an $L \times L$ complex matrix.

In light of Eq. (8), the component energy index is given as follows. First, use eigenvalues $\{\lambda_j|j = 1, \ldots, N\}$ to construct base vectors which are grouped into a matrix E:

$$E = [\Lambda_1 \ \Lambda_2 \cdots \Lambda_N], \tag{9}$$

where $\Lambda_j = (1 \ \lambda_j \cdots \lambda_j^{q-1})^{\mathrm{T}}$, $j = 1, \ldots, N$. Next, compute $\upsilon = (\mathrm{tr}(\hat{r}(1)) \ \mathrm{tr}(\hat{r}(2)) \cdots \mathrm{tr}(\hat{r}(q)))^{\mathrm{T}}$, where $\mathrm{tr}(\cdot)$ denotes the trace of a matrix, and expand υ with respect to the vectors $\{\Lambda_j|j = 1, \ldots, N\}$:

$$\upsilon = \sum_{j=1}^{N} \Lambda_j F_j = EF, \tag{10}$$

where $F = (F_1\ F_2 \cdots F_N)^{\mathrm{T}}$ is a complex vector. Then, solve Eq. (10) and extract the components from υ:

$$F = E^{+}\upsilon,$$
$$\varepsilon_j = \Lambda_{2j-1}F_{2j-1} + \Lambda_{2j}F_{2j}, \quad j = 1, 2 \ldots, N/2, \tag{11}$$

where E^{+} is the generalized inverse of E and ε_j is a component of υ. Finally, define the energy index as

$$\mathrm{CEI}(j) = \sqrt{\varepsilon_j^{\mathrm{H}}\varepsilon_j}, \quad j = 1, 2, \ldots, N/2, \tag{12}$$

where CEI(j) is the jth component energy index and the superscript H denotes complex conjugate and vector transpose. As we know, the Fourier spectrum of υ can give energy information of all modes, but there may exist large errors in the spectrum peak positions due to the limited frequency resolution. In contrast, CEI can indicate the energy contribution of each mode at a frequency closer to the exact one.

3. An alternative stabilization diagram

The order stabilization diagram is devised to reflect the variation of estimates with order increments. With the increase in model order, the number of spurious modes also increases, which may result in increasing interference of spurious modes. In practice, estimates depend not only on model order but also on the correlation sequence $\{\hat{r}(i)|i \geqslant 0\}$ as defined by Eq. (4). With more $\hat{r}(i)$ appended to the Hankel matrix $\hat{R}$, spurious modes will have large variations in frequency and damping ratio. When model order is fixed, the variation of estimates with row increments of $\hat{R}$ constitutes another form of stabilization diagram. To obtain this form of diagram, we give the following procedure:

(i) Estimate model order in terms of CEI. Suppose the order is n, greater than the system order N.
(ii) Construct a submatrix $\hat{R}(1 : \beta L, 1 : n)$ from $\hat{R}$, β is an index number and satisfies $\beta L > N$.
(iii) Compute the QR decomposition of $\hat{R}(1 : \beta L, 1 : n)$. Suppose $\hat{R}(1 : \beta L, 1 : n) = \overline{QR}$.
(iv) Estimate C, A form $\overline{Q}$ according to Eq. (6), i.e.

$$C = \overline{Q}(1 : L, 1 : N),$$

$$A = \overline{Q}^{+}(1 : (\beta - 1)L, 1 : N)\overline{Q}(L + 1 : \beta L, 1 : N).$$

(v) Compute frequencies, damping ratios and normalized mode shapes according to Eq. (7).
(vi) Increase index β ($\beta + 1 \to \beta$) and go to step (ii).

Using QR decomposition instead of SVD in the above procedure is to reduce computation complexity. In general, QR decomposition can give the range space of $\hat{R}(1 : \beta L, 1 : n)$ except in extreme cases where the rank deficiency of $\hat{R}(1 : \beta L, 1 : n)$ cannot be found. The feature of the

above procedure is that the number of spurious modes is less than the assumed model order n and step (iii) can be realized in a recursive style [20].

In the following sections, examples on model order estimation and modal parameter identification are given to demonstrate the efficacy of CEI and stabilization diagram.

4. Numerical examples

4.1. Order estimation of a system with closely spaced modes

Consider a system whose free response comprises four exponentially decayed components:

$$y(t) = \exp(-15t)\cos(100\pi t) + \exp(-30t)\cos(101\pi t) + \exp(-45t)\cos(102\pi t) + \exp(-60t)\cos(103\pi t).$$

Eigenvalues of the system are -2.3873 ± 50.0i, -4.7746 ± 50.5i, -7.1620 ± 51.0i and -9.5493 ± 51.5i. To estimate these eigenvalues from $y(t)$, 1000 points are sampled at the rate of 500 Hz and a 12th order model is used. Table 1 gives the estimated results. As shown in the table, eigenvalues are accurately estimated. The important result is that singular values of the Hankel matrix $\hat{R}$ as defined by Eqs. (4) and (5) cannot give a clear order indication, whereas CEIs definitely indicate that there are four dominant modes, which implies that using singular values may yield an underestimated order when there exist closely spaced modes. In the table, every eigenvalue is connected with an index from which we can know the energy contribution of the corresponding modal vibration. Therefore, the efficacy of CEI in this example is obvious.

Table 1
CEIs and singular values

No.	Estimated eigenvalue	CEI	Singular value
1	$-2.3873 \pm 50.0i$	66.516	256.58
			241.34
2	$-4.7746 \pm 50.5i$	34.140	5.7081
			3.7479
3	$-7.1620 \pm 51.0i$	22.531	0.0261
			0.0103
4	$-9.5493 \pm 51.5i$	16.310	9.6044e−006
			2.8491e−006
5	−35.811 ± 194.14i	1.03×10^{-7}	6.8769e−014
			5.0699e−014
6	−16.726 ± 197.27i	8.29×10^{-8}	2.2156e−014
			1.1655e−014

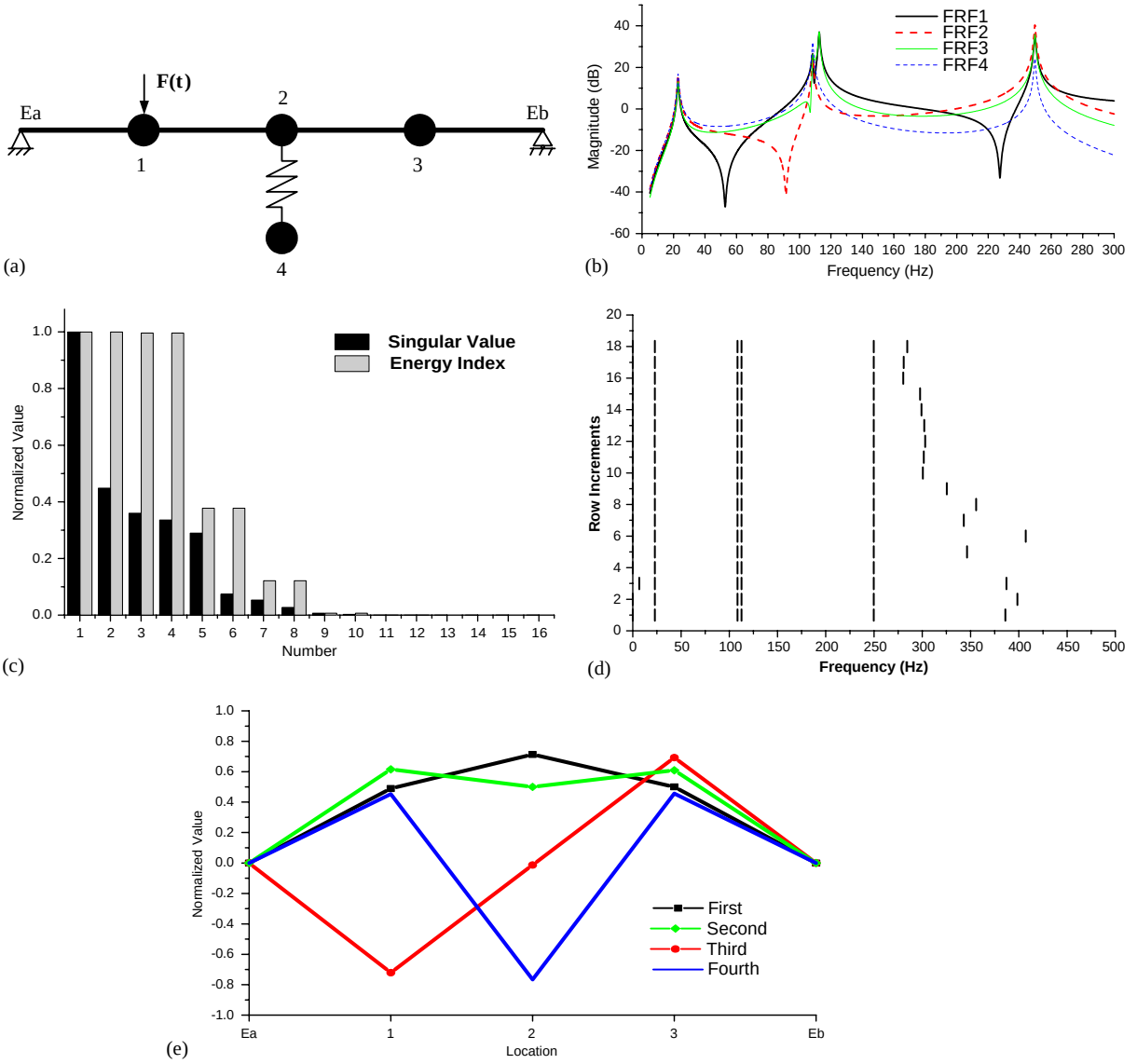

Fig. 1. (a) A vibration system with four masses. (b) Frequency response functions. (c) Normalized singular values and CEIs. (d) Stabilization diagram. (e) Estimated mode shapes of the beam.

4.2. *Parameter estimation of a system of 4 degrees of freedom*

Consider a vibration system that consists of a lumped beam and a vibration absorber (Fig. 1(a)). Stiffness of the absorber is elaborately adjusted so that there are two closely spaced modes. Natural frequencies of the system are 22.86, 108.45, 112.54 and 249.67 Hz. The whole system is lightly damped and damping ratios of the four modes are 0.017, 0.0037, 0.0035 and 0.0016 (in ascending order). To identify mode shapes of the beam, white noise excitation is loaded

Table 2
Estimated frequencies and damping ratios

Order	1	2	3	4
Frequency (Hz)	22.89	108.53	112.69	249.71
Damping ratio	0.019	0.0038	0.0047	0.0013

at Mass 1 and acceleration responses of masses 1–3 are measured simultaneously. The sampling rate is 1000 Hz and 8192 samples/channel are collected. FRFs corresponding to the four masses are given in Fig. 1(b), from which we can see that the third mode is unobservable at masses 2 and 4. To give an order estimate, a 16th order model is initially used. The comparison of normalized singular values and CEIs (Normalization is defined as dividing each singular value and CEI by the maximum singular value and CEI, respectively) is given in Fig. 1(c), which illustrates that CEI is more effective in order indication than singular value. Since the model is redundant, spurious modes are inevitable. Although the first four pairs of CEIs in Fig. 1(c) correspond to the four natural modes, in order to further verify that there are no more physical modes, stabilization diagram is also applied to show the variation of estimated frequencies. Fig. 1(d) is the frequency stabilization diagram which is derived from a 12th-order model. In the figure, spurious and physical modes are clearly separated, which demonstrates the 12th-order model is sufficient. Table 2 gives the estimated parameters which are very close to the exact values. Estimated mode shapes are shown in Fig. 1(e), which also illustrate that the third mode is unobservable at masses 2 and 4 since mass 2 is located exactly at the node position.

5. Parameter identification of a cable-stayed bridge model

5.1. Measurement and excitation of the bridge model

The bridge model as shown in Fig. 2(a) has two bridge towers and 40 steel cables. Distance between the two towers is 2000 mm and the model span is 4000 mm. In order to identify bending and torsional modes of the bridge model, 14 accelerometers were symmetrically placed on the bridge body and one shaker was used to give white noise excitation (Fig. 2(b)). The longitudinal distance between any two adjacent accelerometers is 600 mm, and the transverse distance is almost the width of the bridge model. The shaker is 200 mm away from the center. At each measurement point, 4096 samples were collected at the rate of 125 Hz.

5.2. Frequency estimation by time–frequency analysis

From the measured data, natural frequencies can be approximately estimated by time–-frequency analysis [21,22]. Time–frequency representation (TFR) can reflect signal components in the time–frequency domain. Using TFR in this example is to give a coarse estimation of natural frequencies as well as to examine whether response signals have time-varying characteristics that

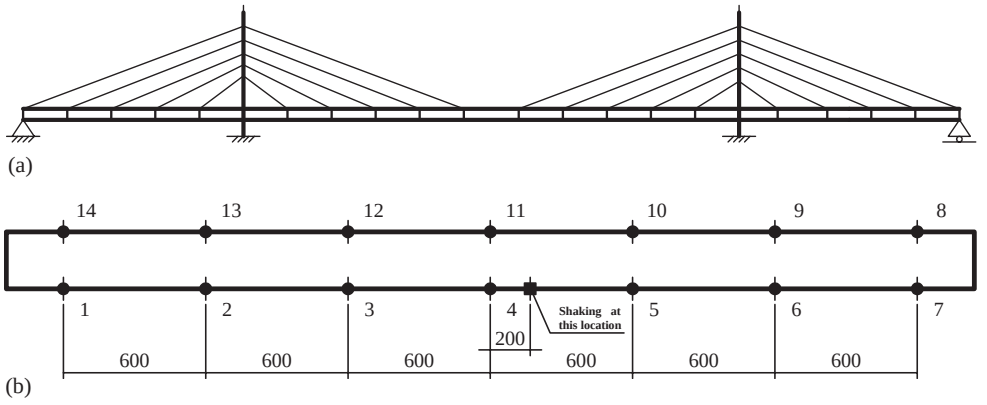

Fig. 2. (a) Sketch of the cable-stayed bridge model. (b) Measurement and excitation locations.

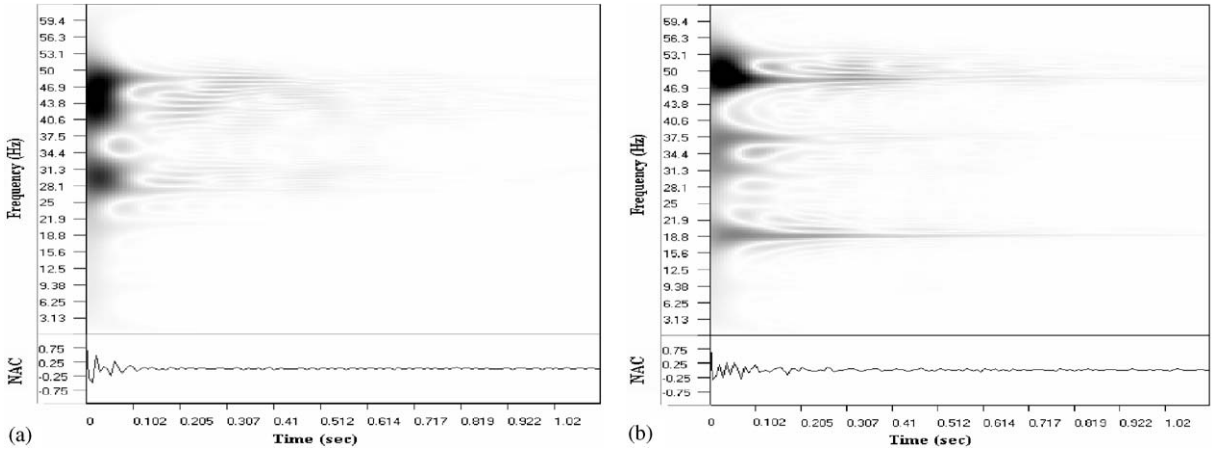

Fig. 3. (a) Time–frequency representation of the normalized autocorrelation sequence of Point 5. (b) Time–frequency representation of the normalized autocorrelation sequence of Point 9.

may be caused by model nonlinearities. Fig. 3(a) and (b) are TFRs of the normalized autocorrelation (NAC) sequences corresponding, respectively, to points 5 and 9. TFRs of other points are similar to these two figures, which indicates the response signals are stationary. From all TFRs of the 14 points natural frequencies are found to be near 9, 19, 25, 27, 31, 37, 43, 48 and 53 Hz.

5.3. Parameter estimation by subspace identification technique

According to the procedure given in Section 3, model order should be estimated at first. To this end, a redundant model of order 40 is used to obtain CEIs. Fig. 4 gives the normalized singular values and CEIs (as defined in Section 4.2). In terms of CEIs, a 36th-order model is shown to be

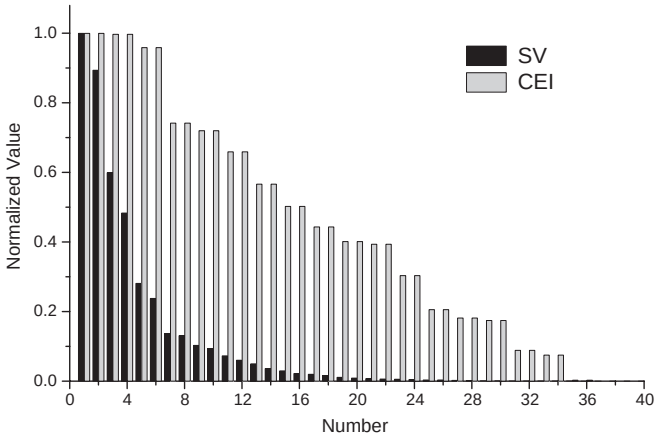

Fig. 4. Normalized singular values and CEIs.

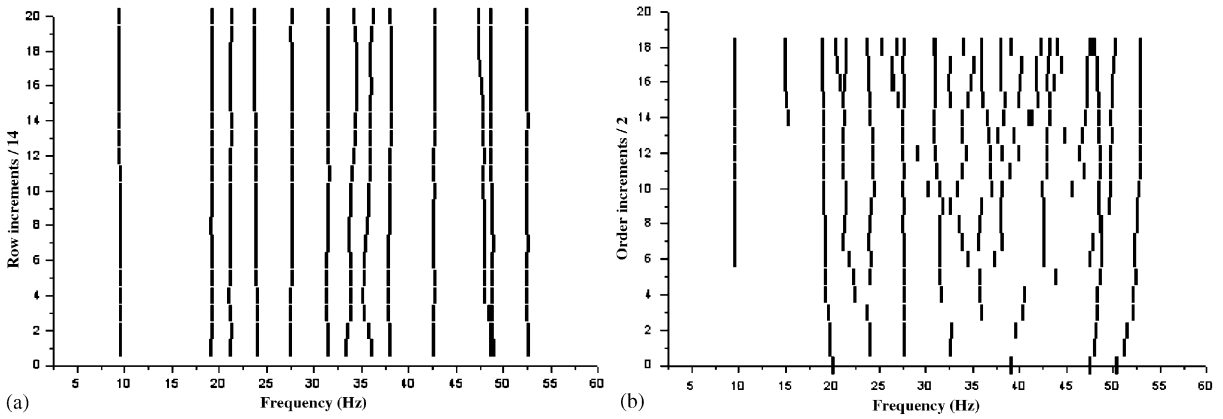

Fig. 5. (a) Stabilization diagram—frequency versus row increments of $\hat{R}(1:\beta L, 1:n)$. (b) Stabilization diagram—frequency versus model order increments.

sufficient to model all signal components. As the model is redundant, there exist many spurious modes in the estimated results. In order to identify and remove these modes, a stabilization diagram is constructed to reflect the variation of estimated frequencies. In Fig. 5(a), 10 of the 13 modes keep almost unchanged to the row increments of the matrix $\hat{R}(1:\beta L, 1:n)$ and those modes with damping ratios greater than 0.1 are not shown. Eigenvalues and CEIs corresponding to the ten "stable" modes are given in Table 3, where CEI is connected with each mode to indicate its energy contribution. Compared with the results given by TFR, the ten modes can be considered reliable. Table 4 gives the estimated frequencies and damping ratios, where the results by FDD technique are also presented as a comparison.

Fig. 5(b) is the diagram where the variation or stabilization of frequencies with model order increments is illustrated. The initial model order is 20 and the maximum order increment is 36. In the diagram, interference of spurious modes appears stronger than that of Fig. 5(a). Generally,

Table 3
Estimated eigenvalues and CEIs

Order	Eigenvalue	CEI
1	$-0.75 \pm 09.56i$	0.1388
2	$-0.74 \pm 19.21i$	0.2222
3	$-1.96 \pm 21.04i$	0.0200
4	$-2.14 \pm 23.93i$	0.2803
5	$-1.21 \pm 27.59i$	0.3038
6	$-1.76 \pm 31.32i$	0.0888
7	$-2.31 \pm 37.80i$	0.1944
8	$-2.30 \pm 42.66i$	0.1203
9	$-1.46 \pm 48.82i$	0.2290
10	$-1.67 \pm 52.47i$	0.1398

Table 4
Estimated natural frequencies and damping ratios

	Frequency (Hz)		Damping ratio	
Order	Subspace identification	FDD	Subspace identification	FDD
1	9.59	9.6	0.078	0.104
2	19.23	19.1	0.039	0.022
3	21.13	—	0.093	—
4	24.03	24.1	0.089	0.067
5	27.62	27.5	0.044	0.061
6	31.37	—	0.056	—
7	37.87	37.7	0.061	0.052
8	42.72	—	0.054	—
9	48.85	48.7	0.030	0.046
10	52.49	—	0.032	—

using a high-order model is necessary to model weakly observable modes but at the same time introduces spurious modes which should be carefully dealt with. The comparison between Fig. 5(a) and (b) shows that the alternative stabilization diagram is more effective in this example.

5.4. Estimated mode shapes

According to the identified results, the bridge model has 10 observable modes within the analysis band. The corresponding mode shapes are illustrated in Fig. 6(a–j). Among these modes, the first is a bending mode and the second mode in fact vibrates up and down (not reflected in the figure). The third mode is also a bending mode but its ends are antisymmetric. The eighth mode is almost a torsional mode and the rest have both bending and torsional deflections. Some of these shapes such as the second are closely related to the vibration of cables, which implies that the cable vibration has a significant effect on the bridge body.

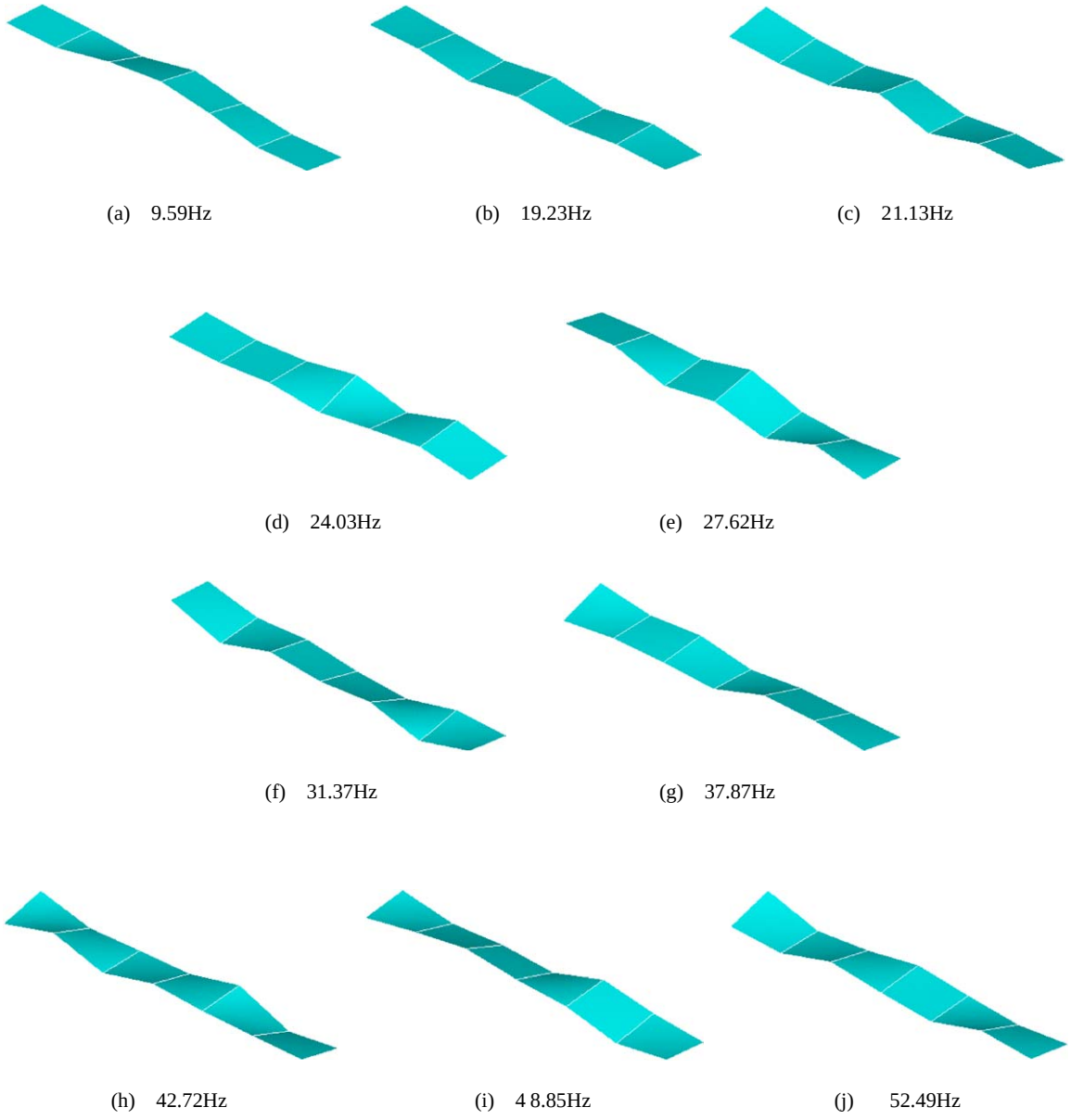

Fig. 6. Estimated mode shapes.

6. Conclusion

It is of great significance to develop techniques for modal parameter identification from response data only. The subspace identification technique has been employed to estimate the modal parameters of a theoretical system as well as a cable-stayed bridge model. Two issues have been addressed in the paper: one is concerned with model order estimation and the other with spurious mode elimination. On order estimation, a new method has been introduced to enhance

the SVD-based order estimation technique, which is realized by connecting each mode with a quantitative index—CEI. Also investigated is an alternative stabilization diagram that reflects the variation of frequencies with the row increments of the Hankel matrix and further indicates spurious estimates. Examples have been presented to demonstrate the efficacy of the proposed methods and results have shown that singular values may indicate an underestimated model order whereas the proposed CEI appears preferable in order estimation. A redundant model inevitably results in spurious modes, but in the identification of modal parameters of the bridge model, spurious modes are completely identified with the help of the alternative stabilization diagram.

Acknowledgements

This work was supported in part by the NSF financed Project No. 10302019.

References

[1] E. Luz, J. Wallsheck, Experimental modal analysis using ambient vibration, *International Journal of Analytical and Experimental Modal Analysis* 7 (4) (1992) 29–39.
[2] B. Peeters, G. De Roeck, Reference-based stochastic subspace identification for out-only modal analysis, *Mechanical Systems and Signal Processing* 13 (6) (1999) 855–878.
[3] P. Bonato, R. Ceravolo, A. De Stefano, F. Molinari, Use of cross time frequency estimators for structural identification in non-stationary condition and under unknown excitation, *Journal of Sound and Vibration* 273 (5) (2000) 775–791.
[4] M. Goursat, M. Basseville, A. Benveniste, L. Mevel, Output-only modal analysis of Ariane 5 launcher, *Proceedings of the 19th IMAC*, Orlando, FL, 2001, pp. 1483–1489.
[5] S. Gouttebroze, J. Lardies, On using wavelet transform in modal analysis, *Mechanics Research Communications* 28 (5) (2001) 561–569.
[6] J. Lardies, N. Larbi, A new method for model order selection and modal parameter estimation in time domain, *Journal of Sound and Vibration* 245 (2) (2001) 187–203.
[7] G.H. James, T.G. Carne, J.P. Lauffer, The natural excitation technique (NExT) for modal parameter extraction from operating structures, *International Journal of Analytical and Experimental Modal Analysis* 10 (4) (1995) 260–277.
[8] S.R. Ibraham, Efficient random decrement computation for identification of ambient responses, *Proceedings of the 19th IMAC*, Orlando, FL, 2001, pp. 698–703.
[9] R. Brincker, L. Zhang, P. Anderson, Modal identification from ambient responses using frequency domain decomposition, *Proceedings of the 18th IMAC*, San Antonio, TX, 2000.
[10] S. Marchesiello, B.A.D. Piomto, S. Sorrentino, Application of the CVA-BR method to the Z24 bridge vibration data, *Proceedings of the 19th IMAC*, 2001, pp. 864–869.
[11] J.N. Juang, R.S. Pappa, An eigen-system realization algorithm for modal parameter identification and model reduction, *Journal of Guidance, Control and Dynamics* 8 (1985) 620–627.
[12] W. Favereel, B. De Moor, P. Van Overschee, Subspace state space system identification for industrial processes, *Journal of Process Control* 10 (2000) 149–155.
[13] L. Mevel, A. Berveniste, M. Berreville, M. Goursat, Blind subspace based eigenstructure identification under nonstationary excitation using moving sensors, *IEEE Transactions on Signal Processing* 50 (1) (2002) 41–48.
[14] L. Ljung, *System Identification: Theory for the User*, Prentice-Hall, Englewood Cliffs, NJ, 1999.
[15] P. Van Overschee, B. De Moor, *Subspace Identification for Linear Systems: Theory-Implementation-Applications*, Kluwer Academic Publishers, Dordrecht, Netherlands, 1996.

[16] L. Zhang, Modal indicators for operational modal identification, *Proceedings of the 19th IMAC*, Orlando, FL, 2001, pp. 746–749.
[17] W. Heylen, S. Lammens, P. Sas, *Modal Analysis Theory and Testing*, Prentice-Hall, Englewood Cliffs, NJ, 1999.
[18] D.G. Manolakis, V.K. Ingle, S.M. Kogon, *Statistical and Adaptive Signal Processing: Spectral Estimation, Signal Modeling, Adaptive Filtering and Array Processing*, McGraw-Hill, New York, 2000.
[19] K. Zhou, J.C. Doyle, K. Glover, *Robust and Optimal Control*, Prentice-Hall, Englewood Cliffs, NJ, 1996.
[20] G.H. Golub, C.F. Von Loan, *Matrix Computations*, 3rd ed., The Johns Hopkins University Press, Baltimore, MD, 1996.
[21] Z.Y. Zhang, H.X. Hua, X.Z. Xu, et al., Modal parameter identification through Gabor expansion of response signals, *Journal of Sound and Vibration* 266 (2003) 943–955.
[22] S. Qian, D.P. Chen, *Joint Time Frequency Analysis—Methods and Application*, Prentice-Hall PTR, Englewood Cliffs, NJ, 1996.